Hybrid III-V on Silicon lasers for photonic integrated circuits on Silicon

Guang-Hua Duan, *Senior Member, IEEE*, Christophe Jany, Alban Le Liepvre, Alain Accard, Marco Lamponi, Dalila Make, Peter Kaspar, Guillaume Levaufre, Nils Girard, François Lelarge, Jean-Marc Fedeli, Antoine Descos, Badhise Ben Bakir, Sonia Messaoudene, Damien Bordel, Sylvie Menezo, Guilhem de Valicourt, Shahram Keyvaninia, Gunter Roelkens, Dries Van Thourhout, David J. Thomson, Frederic Y. Gardes, and Graham. T. Reed

(Invited Paper)

***Abstract*—This paper summarizes recent advances of integrated hybrid InP/SOI lasers and transmitters based on wafer bonding. At first the integration process of III-V materials on silicon is described. Then the paper reports on the results of single wavelength distributed Bragg reflector lasers with Bragg gratings etched on silicon waveguides. We then demonstrate that, thanks to the high-quality silicon bend waveguides, hybrid III-V/Si lasers with two integrated intra-cavity ring resonators can achieve a wide thermal tuning range, exceeding the C band, with a side mode suppression ratio higher than 40 dB. Moreover, a compact array waveguide grating on silicon is integrated with a hybrid III-V/Si gain section, creating a wavelength-selectable laser source with 5 wavelength channels spaced by 400 GHz. We further demonstrate an integrated transmitter with combined silicon modulators and tunable hybrid III-V/Si lasers. The integrated transmitter exhibits 9 nm wavelength tunability by heating an intra-cavity ring resonator, high extinction ratio from 6 to 10 dB, and excellent bit-error-rate performance at 10 Gb/s.**

***Index Terms*— Hybrid photonic integrated circuits, silicon laser, semiconductor lasers, silicon-on-insulator (SOI) technology, adiabatic taper.**

I. Introduction

Silicon photonics is attracting a lot of attention due to the prospect of low-cost, compact circuits that integrate photonic and microelectronic elements on a single chip [1,2]. It can address a wide range of applications from short-distance data communication to long-haul optical transmission [3]. Today, practical Si-based light sources are still missing, despite the recent promising demonstration of an optically pumped germanium laser [4,5]. This situation has propelled research on heterogeneous integration of III-V semiconductors with silicon through wafer bonding techniques [6-8]. In this approach, unstructured InP dies or wafers are bonded, epitaxial layers facing down, on an SOI waveguide circuit wafer, after which the InP growth substrate is removed and the III-V epitaxial film is processed. Such an approach exploits the highly efficient light emission properties of some direct-gap III-V semiconductor materials such as compounds based on GaAs and InP.

Important achievements have been made in the past on the heterogeneous integration of III-V on silicon as reported in [6-8]. Two different waveguide structures for the hybrid III-V/Si integration have been investigated. In the first one, as described in [6] and [8], the mode is mainly guided by the Si waveguide and evanescently couples with the III-V waveguide, using a very thin bonding layer (< 5 nm, corresponding to the Si native oxide). In the second one described in [7], the mode in the hybrid section is mainly guided by the III-V waveguide, and the light is coupled from the III-V waveguide to the silicon waveguide through waveguide tapering. In this case, the bonding interface can be relatively thick (from 30 to 150 nm, typically). The advantage is that the optical mode experiences a high optical gain in the central region of the laser structure. This paper will focus on the second waveguide structure, and will demonstrate that efficient mode transfer can be achieved between III-V and silicon waveguide [9,10]

Large progress have also been made in the past on the emission spectrum control. For instance, distributed feedback (DFB) and distributed Bragg reflector (DBR) lasers with single longitudinal mode emission have been reported in [8]. In those lasers, the Bragg gratings are etched on silicon waveguides by keeping the III-V waveguide as simple as possible. More recently, wavelength tunable lasers with large tuning range have been published, showing very promising

This work was supported in part by the European FP7 Helios project, and the French national ANR projects Micros, Silver and Ultimate.

G.-H. Duan, C. Jany, A. Leliepvre, A. Accard, M. Lamponi, D. Make, P. Kaspar, G. Levaufre, N. Girard and F. Lelarge are with III-V Lab, a joint lab of 'Alcatel-Lucent Bell Labs France', 'Thales Research and Technology' and 'CEA Leti', Campus Polytechnique, 1, Avenue A. Fresnel, 91767 Palaiseau cedex, France.

J.-M. Fedeli, A. Descos, B. Ben Bakir, S. Messaoudene, D. Bordel, and S. Menezo are with III-V Lab, a joint lab of 'Alcatel-Lucent Bell Labs France', 'Thales Research and Technology' and 'CEA Leti', LETI, Minatec, 17 rue des Martyrs, F-38054 GRENOBLE cedex 9, France.

G. de Valicourt is with Bell Laboratories, WDM Dynamic Networks Department, Centre de Villarceaux, Route de Villejust, 91620, Nozay, France

S. Keyvaninia G. Roelkens, and D. Van Thourhout are with Photonic Research Group, INTEC, Ghent University-IMEC, Sint-Pietersnieuwstraat 41, B-9000 Ghent, Belgium.

D. J. Thomson, F. Y. Gardes and G. T. Reed are with Optoelectronics Research Centre, University of Southampton, Southampton, Hampshire, SO17 1BJ, UK

results [11,12,13]. We demonstrate that the use of two silicon ring resonators allows us to achieve a tuning range of more than 45 nm and a side mode suppression ratio (SMSR) larger than 40 dB over the entire tuning range [11].

Thanks to the mature silicon fabrication process, even more complicated silicon waveguides structures can be integrated within a hybrid III-V/Si laser and used for laser wavelength control. For instance, an arrayed waveguide grating (AWG) filter can be integrated in a laser cavity, together with several semiconductor optical amplifiers (SOA), in order to make an AWG laser. The first AWG laser on Si was reported in [14] with 4 channels spaced by 360 GHz. The threshold current ranged from 113 to 147 mA, and the output power to a fibre from -23 to -14.5 dBm. We recently demonstrated a 5-channel AWG laser with 392 GHz separation [15], and also a 4channel AWG laser with 200 GHz channel spacing [16]. The threshold current ranged from 38 to 42mA, and the output power in a single-mode fibre from -8.4 to -2.2 dBm.

Integrated transmitters incorporating lasers and modulators on silicon are of primary importance for all communication applications, and at the same time are the most challenging to fabricate due to the need of hybrid III-V integration. The first demonstration of such a photonic integrated circuit (PIC) was reported by A. Alduino *et a*l. [17]. This silicon PIC transmitter is composed of hybrid III-V/silicon lasers and silicon Mach-Zehnder modulators (MZM) operating in the wavelength window of 1.3 µm. However, wavelength-division-multiplexing applications usually require wavelength-tunable laser sources. Moreover, tunable transmitters are considered to be an attractive option in optical network terminal transceivers for future access networks. The very large market of access networks provides an opportunity for silicon photonics. We reported for the first time on an integrated tunable laser MZM (ITLMZ) operating in the wavelength window of 1.5 µm, which combines a tunable hybrid III-V/Si laser and a silicon MZ modulator [18]. Our ITLMZ demonstrates several new features: i) wavelength tunability over 9 nm; ii) a silicon modulator with high extinction ratio (ER) between 6 and 10 dB, and 3 dB modulation bandwidth as large as 13 GHz; and iii) excellent bit-error rate (BER) performance.

This paper will summarize our recent advances on integrated hybrid InP/SOI lasers and transmitters based on wafer bonding. It is organized as follows. Section II is devoted to the heterogeneous integration process of III-V material on silicon, including one of the key points of hybrid III-V/Si lasers: the optical mode transition from III-V to silicon waveguides. Section III gives the results of single-wavelength DBR lasers with high output power. Section IV will focus on wavelength-tunable lasers, and Section V on wavelength-selectable AWG lasers. Section VI reports on the performance of an ITLMZ operating at 10 Gb/s. Finally, a conclusion is drawn in section VII.

II. Heterogeneous Integration of III-V on Silicon

A. Heterogeneous integration process of III-V material on silicon

Figure 1 outlines the process flow for silicon PICs using the heterogenous integration of III-V material on Si.

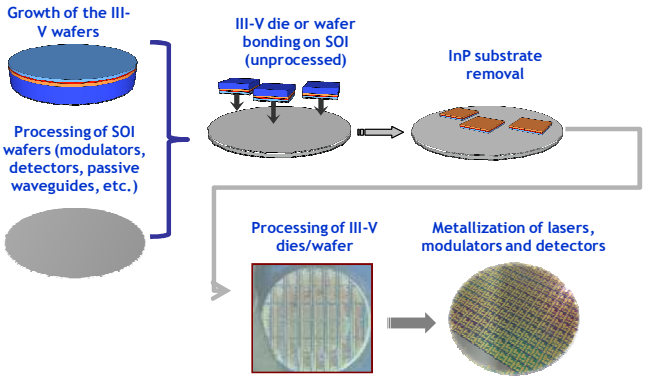

Figure 1 process flow of heterogeneous integration of III-V on silicon

The fabrication starts with 200mm SOI wafers with a typical thickness of 440 nm thick silicon top layer. The first step is the formation of passive rib waveguides by etching the top silicon layer. These waveguides are optimized for the coupling with III-V waveguides that will be aligned on top of the silicon waveguides in a later step. After this etching step, the remaining silicon layer has a thickness of 220 nm. For the passive circuitry, additional etching steps are applied to form strip waveguides and other elements such as Bragg reflectors or vertical output couplers. To planarize the surface of the SOI wafer, a silica layer is deposited and a chemical-mechanical polishing is applied [19].

In the meantime, 2'' InP wafers are grown. The III-V region consists of a p-InGaAs contact layer, a p-InP cladding layer, typically 6 InGaAsP quantum wells surrounded by two InGaAsP separate confinement heterostructure layers, and an n-InP layer. Optimized growth conditions have been established in order to simultaneously achieve a defect-free surface morphology required for bonding and high laser performances. These InP wafers can now be bonded onto the SOI wafers [20].

After wafer bonding and InP substrate removal, dry etching is used to etch through the InGaAs layer and partly etch the InP p-doped waveguide cladding layer. The InP etching is completed by chemical selective etching. The MQW layer is etched by CH_4:H_2 RIE. Figure 2 shows a scanning electron microscope (SEM) picture of a III-V waveguide on top of a silicon waveguide.

The active waveguide is encapsulated with DVS-benzocyclobutene (BCB). A Ti/Pt/Au alloy is used for metallization on both p and n sides. Finally, the fabricated lasers are ready to be tested on the wafer through the use of vertical grating couplers.

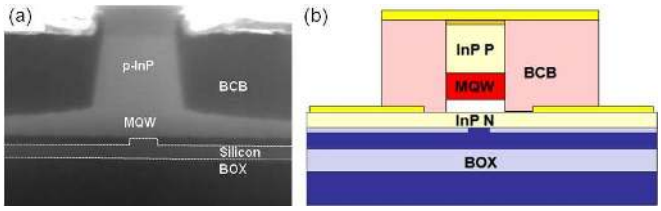

Figure 2: (a) Cross-sectional SEM picture of a hybrid waveguide with white lines added to make the silicon waveguide visible; (b) schematic cross section.

B. Adiabatic coupling between III-V and silicon waveguides

Fig. 3 gives a schematic view of the laser structure, which can be divided into three parts. In the center of the device the optical mode is confined to the III-V waveguide, which provides the optical gain. At both sides of this section there is a coupling region that couples light from the III-V waveguide to the underlying silicon waveguide. After the coupling region the light is guided by a silicon waveguide without III-V on top.

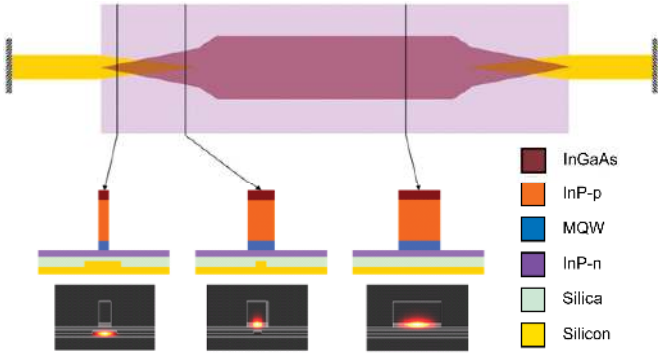

Figure 3 Top and cross-sectional views of the coupling structure of the hybrid laser with representative mode profiles in three cross-sections

The intensity profiles of the fundamental mode are calculated using the film mode matching method, and are given in Fig. 3 at different points of the laser cavity. The calculated optical confinement in the MQW layer in the center of the laser cavity is in the range between 5% and 12%.

To achieve index matching between the two waveguides, a deep ridge III-V waveguide is usually used in the double taper region. As shown in Fig. 3, a double taper structure is used to allow the efficient coupling of the fundamental mode from the III-V waveguide to the silicon waveguide [10]. In the right double taper region, the silicon waveguide has an increasing width, while the III-V waveguide's width is decreasing. Figure 4 shows the coupling efficiency of the double adiabatic taper for three values of the III-V tip width: 0.4, 0.8 and 1 µm and a silicon waveguide thickness of 400 nm. We can see that perfect coupling can only be achieved using a tip width of 0.4 µm or less. This requirement on the tip width is linked to the 400 nm silicon waveguide thickness. For thicker silicon waveguides a larger tip width can be tolerated. We can also observe highly efficient coupling for short taper length (around 30 µm). However, the coupling efficiency varies quickly with the taper length and other parameters for such a short taper. Longer (> 100 µm) tapers are preferred in order to get more robust coupling.

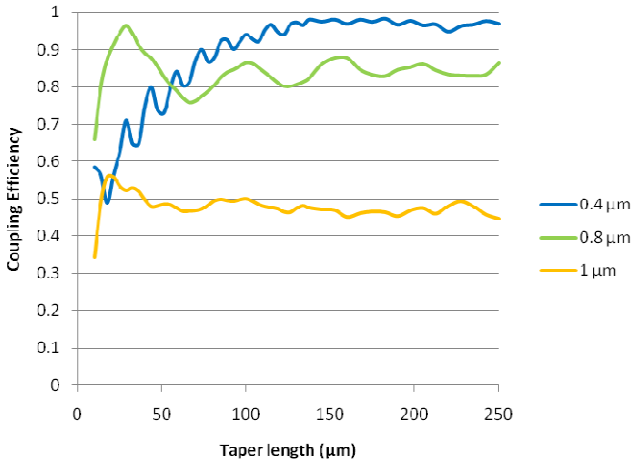

Figure 4: Coupling efficiency for different III-V taper tip widths as a function of the double taper length

In the case of thicker silicon waveguides (≥ 500 nm), only the silicon waveguide needs to be tapered for the mode-transfer from the III-V waveguide to the silicon waveguide [9]. As narrow III-V tapers are no longer required, the process of III-V waveguides becomes much more tolerant.

III. SINGLE MODE DBR LASERS

A. DBR laser structure

In this section, we report on the experimental demonstration of a heterogeneously integrated III-V/Si DBR laser with low threshold (< 20 mA) and high output power (> 15 mW). The laser performances are similar to those obtained by A. J. Zilkie *et al*. who built a hybrid external-cavity DBR laser from a III-V reflective SOA butt-coupled to a 3 µm-thick Si waveguide containing a Bragg grating reflector [21].

The optical cavity is defined by a III-V gain section of 400 µm length and two DBRs spaced 600 µm apart, as shown in Fig. 5. The Bragg grating was etched into a silicon waveguide with a width of 10 µm. The grating pitch is 237nm and the duty cycle is 50%. The etching depth is chosen to be only 10 nm, resulting in a reasonable grating coupling coefficient, κ, of 83 cm^{-1}. The back-side Bragg grating has a length of 300 µm, leading to a calculated modal reflectivity of 97.3% and a 3 dB bandwidth of 2.58 nm. The front-side Bragg grating has a length of 100 µm. From calculation, this Bragg grating has a modal reflectivity of 46.4% and a 3 dB bandwidth of 3.98 nm. The combined Bragg gratings lead to a sufficiently narrow filter to allow single longitudinal mode operation of the DBR laser.

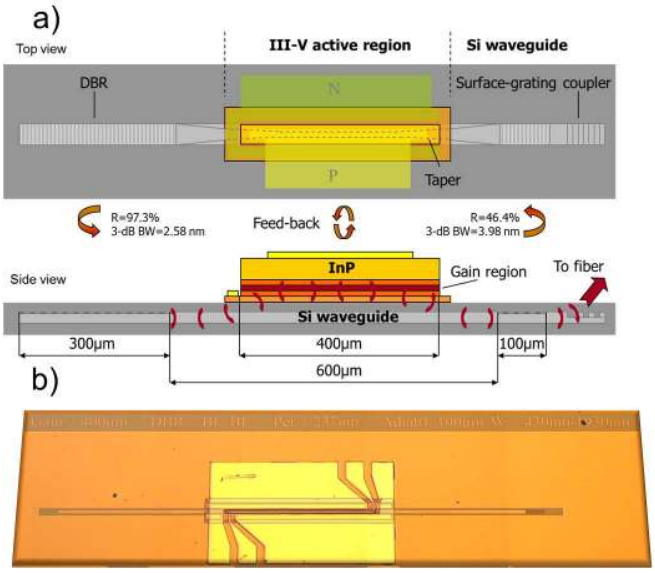

Figure 5: a) Schematic representations of the hybrid III-V/Si laser, top and side views. b) Optical microscope image of the final fabricated device.

B. *Experimental results*

The continuous wave laser output power is collected through a surface-grating coupler by a multimode fiber and then characterized by using both a spectrum analyzer and an optical power meter. To determine the output power at the low-reflectivity side of the hybrid DBR laser, we measured the insertion losses using a reference structure on the same wafer.

Figure 6 shows the fiber-coupled and front mirror output power-current *(L-I)* characteristics for operating temperatures ranging from 15 to 65 °C. As can be seen from the *L-I* curves, the laser threshold is 17 mA with a maximum output power of 15 mW at 20 °C (> 4 mW in the fiber), leading to a differential efficiency of 13.3 %. The differential efficiency is defined as the derivative of the L-I curve, multiplied by e/hν, with e the electron charge and hν the photon energy. It operates up to a stage temperature of 60 °C with a front mirror output power exceeding 2.4 mW.

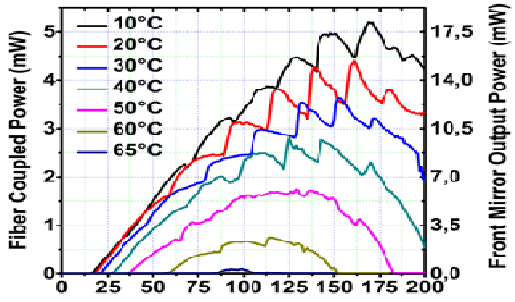

Fig. 6: L-I characteristics of the hybrid DBR laser for different temperatures.

The lasing spectrum for a drive current of 118 mA is shown in Fig. 7. We can see that there is a dominant mode at 1546.97 nm, with a SMSR of about 50 dB.

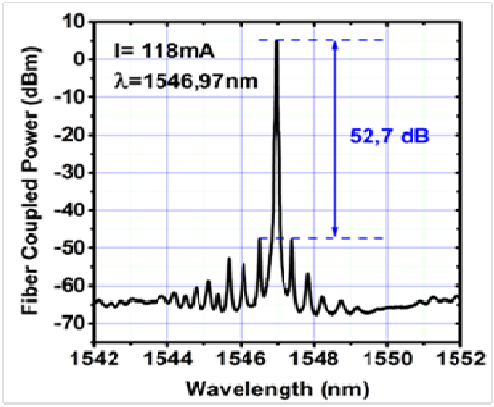

Fig. 7 Lasing spectrum measured at a bias current of 118 mA

Figure 8 shows the lasing spectrum as a function of the drive current along with the corresponding *L-I-V* curves. Measurements were performed at room temperature. We can see that the device has a lasing turn-on voltage of 1.0 V and a series resistance of 7.5 Ω. From the optical spectrum, we can clearly observe jumps in the lasing longitudinal mode due to mode hops. This is due to the fact that the increase of the injection current into the gain section results in an increase of the temperature of the III-V waveguide. Consequently the refractive index of the III-V materials increases, leading to a red shift of the longitudinal mode of the hybrid DBR laser. When the lasing mode is far enough from the reflectivity peak, the dominant longitudinal mode hops to another mode closer to the reflection peak of the Bragg grating.

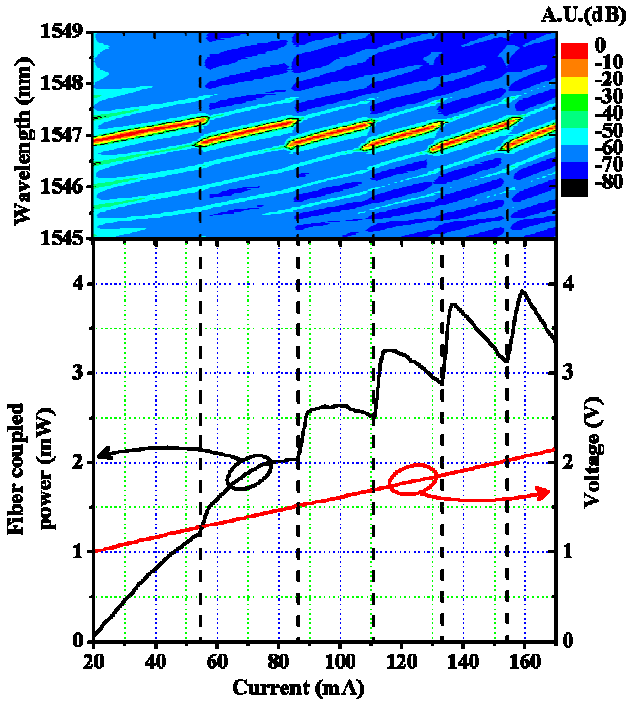

Fig. 8: Fiber-coupled L-I-V characteristic and normalized contour plot of the lasing spectra at room-temperature.

The small-signal modulation response of the laser is shown in Fig. 9. One can observe a flat response at low frequencies and also resonance due to relaxation oscillations. The 3 dB

bandwidth of around 7 GHz is obtained for bias currents ranging from 125 mA to 150 mA.

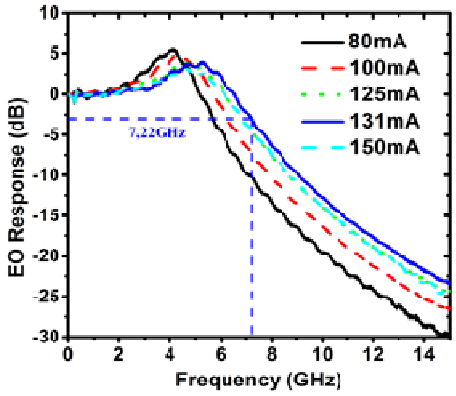

Fig. 9 Room-temperature frequency response of the hybrid DBR laser for different bias currents.

IV. WAVELENGTH TUNABLE LASERS

A. *Design and fabrication*

The tunable laser, as schematically shown on Fig 10 (top), consists of an InP-based amplification section, tapers for the modal transfer between III-V and Si waveguides, two ring resonators (RR) for single mode selection, metal heaters on top of the rings for the thermal wavelength tuning and Bragg gratings providing reflection and output fibre coupling. The straight III-V waveguide has a width of 1.7 µm and a length of 500 µm. In the silicon sections, ring resonator 1 (R1) and 2 (R2) have a free spectral range (FSR) of 650 and 590 GHz, respectively. The slight difference between these two values allows taking advantage of the Vernier effect for the wavelength tuning. Moreover, the bandwidth of the double ring filter is designed to select only one Fabry-Perot mode of the cavity. The Bragg reflectors are made by partially etching the silicon waveguide. The two Bragg reflectors, each with a pitch of 290 nm and 60 periods, are designed to have a reflectivity of more than 90%, and a 3 dB bandwidth larger than 100 nm.

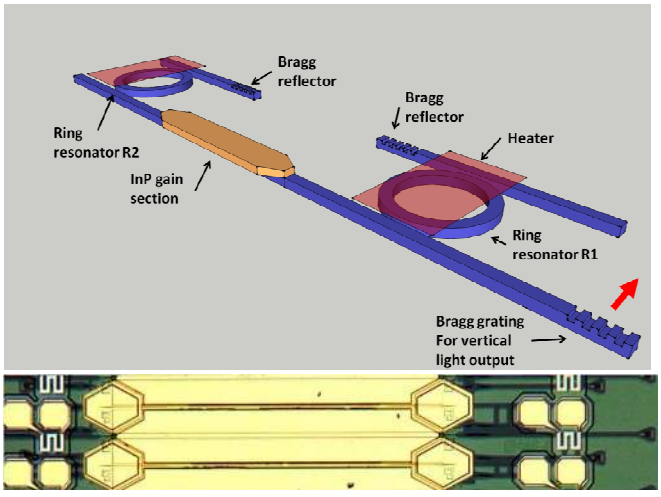

Figure 10: Schematic view (top) and photograph (bottom) of the widely tunable single-mode hybrid laser

In addition to the fabrication steps detailed in Section II, a NiCr metal layer is deposited on top of the ring resonators with contacts pads. This is to allow tuning of the RR wavelength via thermo-optic effect by heating the silicon waveguides. The last steps are the metallization for the laser contacts and heater contacts. Fig. 10 (bottom) shows a picture of the fabricated tunable lasers.

B. *Testing of passive circuit elements*

The passive ring resonators were measured on separated test samples on the same wafer area. Fig. 11 shows the transmission curves of the two RRs from the input port to the "through" port. Two combs of resonance peaks are observed, corresponding to the two RRs with slightly different FSRs. It is remarkable that for each resonance peak, the full width at half minimum is estimated to be around 0.5 nm. Such narrow resonance peaks show the high quality of the fabricated silicon waveguides, and are key to achieve a large tuning range with high SMSR. It is to be noted that the amplitude variation in the presented curves is due to the limited resolution bandwidth (0.07 nm) of the optical spectrum analyzer used.

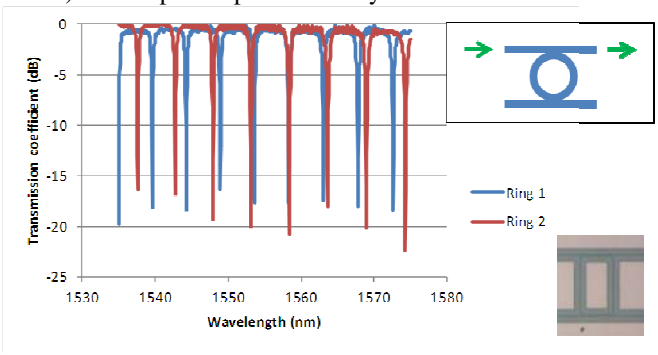

Figure 11: Measured transmission spectra of the ring resonators. Inset: photo of the fabricated silicon ring resonator.

C. *Laser measurements*

The lasers are tested on wafers with vertical Bragg gratings coupling the output light into a cleaved single-mode fiber. The coupling losses were measured to be around 10 dB. At 20°C, the laser has a threshold current of 21mA. Figure 12 shows the laser spectrum at 20°C for a current of 80mA, measured by heating the RRs. It clearly shows single-mode operation with 50 dB SMSR. Such a large SMSR is attributed to the narrow bandwidth of the RRs.

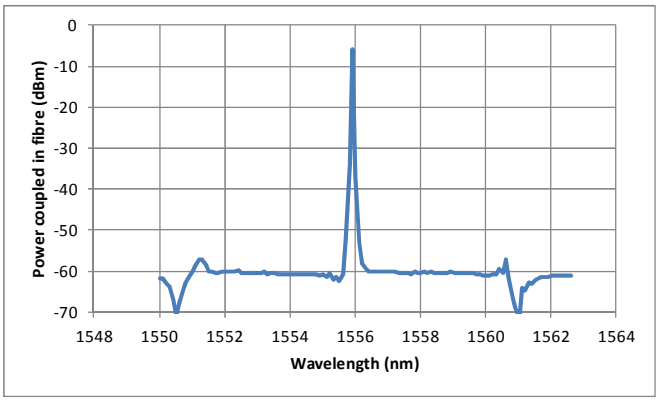

Figure 12 Laser emission spectrum at 20°C, 80mA

The laser linewidth was measured using a self-homodyne technique and also by a heterodyne technique through the beating with an external cavity laser. We found that the linewidth varies with the current injected into the gain region, and with the heating power applied to the RRs. Its values are in the range between 1 and 10 MHz. Figure 13 shows a typical example of the measured heterodyne spectrum, with a Lorentzian fit. We can see that the lineshape is very close to a Lorentzian, and the linewidth is found to be 2.3 MHz.

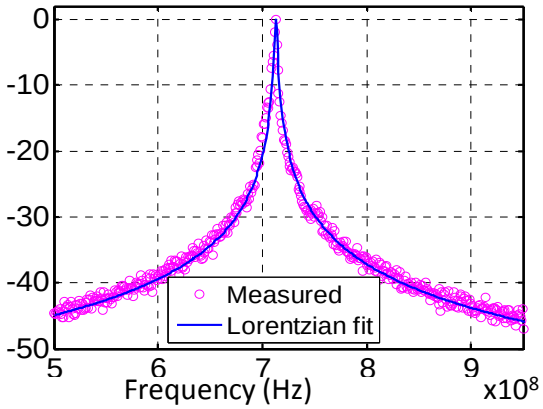

Figure 13: Measured heterodyne spectrum through the beating with an external cavity lasers. A Lorentzian fit is also plotted.

Figure 14 shows the superimposed laser emission spectra obtained by changing heating power levels applied to the two RRs. On the backgrounds of these spectra, as well as on that of Fig. 12, one can observe transmission peaks created by R2 and transmission dips created by R1. This is due to the fact that the spontaneous emission generated by the active III-V waveguide is modulated by the drop transmission of R2 and by the through transmission of R1. The power variation across the wavelength range is 6 dB and corresponds to the gain curve of the III-V material and the vertical coupler spectrum.

Figure 15 shows the wavelength tuning curves of the laser by heating simultaneously the two RRs with a laser injection current of 80 mA at 20°C. With less than 400 mW of combined power in both heaters, a high SMSR (>40dB) wavelength range over 45nm is achieved. For a given power P1 in heater 1, as the power P2 in heater 2 increases, the ring peak wavelengths shifts, and the laser wavelength jumps to the next ring interference order for which the two ring resonance peaks match. For wavelength setting, both ring power must be adjusted so that one transmission peak of R1 matches the one of R2 at a desired wavelength. The wavelength tuning range is currently limited by the too large difference in the FSR between the two RRs. An optimized design should allow covering the whole gain bandwidth of the III-V active material. Also, the laser does not have a phase section and hence the wavelength is always bound to a Fabry-Perot mode of the cavity. For a more precise wavelength tuning (<0.2nm), this laser requires adjusting of the injection current.

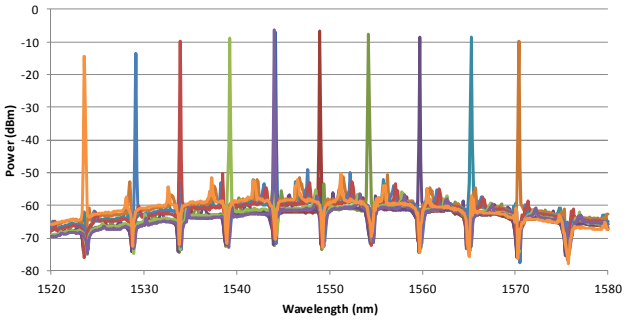

Figure 14: Superimposed laser spectra for different currents injected into heater 1, at 20°C, laser injection current of 80mA. Current applied to heater 2 was fixed.

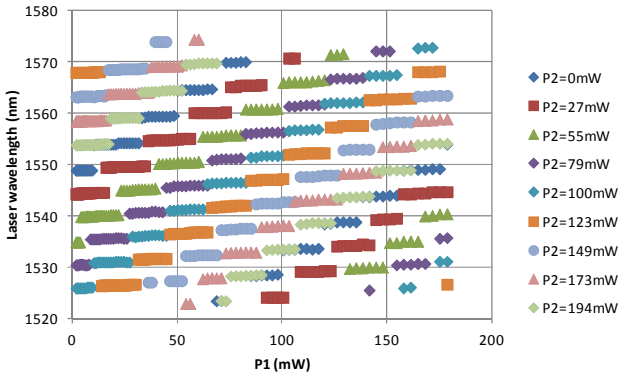

Figure 15:Laser wavelength as a function of the electrical power in heater 1, for different electrical powers in heater 2, at 20°C and laser injection current of 80mA

We demonstrated that such a hybrid III-V/Si laser can be directly modulated at 10 Gb/s [22], an interesting feature for access and metropolitan networks. Moreover, we demonstrated that such a laser can be used as a local oscillator in a coherent receiver for polarization division multiplexing-quadrature phase shift keying signal at 100 Gbit/s [22]. No penalty was observed compared to a commercially available external cavity tunable laser. Those results constitute an important milestone towards real applications of tunable hybrid III-V/Si lasers.

V. AWG-Laser Design and Fabrication

A. *Design*

First AWG lasers on an InP substrate were reported in 1996 [23,24]. However hybrid III-V/Si integration brings new advantages for AWG lasers. As silicon based AWGs [25] have

a reduced size compared to those on InP due to the high refractive index contrast, the laser cavity becomes shorter. For instance, although deeply etched InP waveguides allowed the fabrication of very compact InP AWG lasers, the laser chip size was still 2x3 mm², as demonstrated in [25, 26]. We report here a hybrid III-V/Si AWG laser with a footprint of 1.4x0.8 mm². As a consequence of the smaller cavity, a high side mode suppression ratio can be easier to achieve.

Figure 16 (top) shows a schematic of the AWG laser structure. The AWG laser consists of an AWG made from silicon on insulator (SOI) waveguides and III-V gain sections. The AWG has a size of 300 x 400 µm². It counts 5 output channels with designed 400 GHz spacing. The designed interference order is 20, with 50 strip waveguides in the array part. To reduce the insertion losses of the filter and minimize the reflections, the tapers between the waveguides and the slab propagation region are etched in two steps [24]. The free spectral range (FSR) is designed to be 46 nm, approximatively the bandwidth of the III-V material gain curve. Such a large FSR allows a single-mode laser operation by preventing the neighboring orders from lasing. The Bragg reflectors that terminate the laser cavity are broadband; consequently they do not participate in the wavelength filtering for single-mode selection. The back reflectors R1 are longer and designed for a 99% reflectivity; the transmitted power through R1 can be used for monitoring purposes. The front reflector R2 is designed for a 30% reflectivity and closes the Fabry-Pérot cavity at the other side. At the output side, a vertical grating coupler is used to couple the output light to a cleaved single-mode fiber.

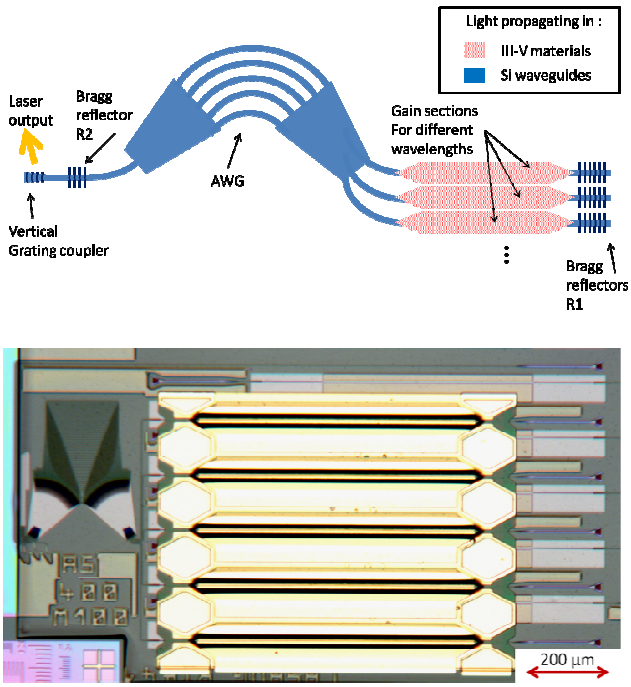

Fig 16 (top) Schematics and (bottom) photograph of a fabricated AWG-laser

B. *Laser Measurements*

The lasers are tested on wafers, using a single-mode cleaved fiber to collect the light that exits the chip through the vertical grating coupler. The test bench temperature is regulated at 20°C. All the measurements are performed using electrical probes. The 5 SOAs of the AWG laser have a series resistance around 7 Ω. Table I shows the main characteristics of each wavelength channel biased at 110 mA. The lasing threshold remains around 40 ± 2 mA for all channels, with the highest threshold corresponding to the lowest wavelength, because this channel has the largest detuning with respect to the peak gain wavelength: 1535 nm. For a given injection current (110 mA), the power coupled to the fibre ranges from -8.63 dBm to -10.93 dBm. The coupling losses from the vertical coupler to a single-mode fiber (SMF) were measured to be in the range of 12-10 dB between 1513 nm and 1525 nm. Therefore, the power in the silicon output waveguide is estimated to be in the range of 1-3 mW. The high loss of the vertical coupler comes from the fact that the laser emission wavelength does not match with that of the maximum transmission. In fact, the coupler has a peak transmission around 1560 nm, and a 3dB passband of 45nm. The power variation with the wavelength channel can be explained by the shift between the AWG filter passband (1513 nm to 1525 nm) and the III-V gain peak around 1535 nm. This detuning is due to the deviation of the fabricated waveguide dimensions with respect to the designed ones. The lasing wavelengths are spaced by 392 GHz on average, with ± 40 GHz deviation. This deviation is due to the Fabry-Pérot mode selections inside the AWG passband.

TABLE I
LASER CHARACTERISTICS AT 20°C FOR THE 5 SECTIONS

Active section number	Threshold (mA)	Power coupled to single mode fibre (dBm). I=110mA	Wavelength (nm) I=110mA	SMSR (dB) I=110mA
1	38	-8.6	1525.33	38
2	39	-8.9	1522.56	33
3	38	-9.5	1519.4	35
4	38	-9.9	1516.4	32
5	42	-10.9	1513.33	30

Figure 17 shows power versus injection current for each wavelength channel biased individually. The irregularities on the curve are due to mode hops. The Fabry-Pérot modes shift with injection current due to temperature effects in the SOA sections, whereas the AWG wavelengths stay constant as the test bench temperature is regulated at 20 °C. Apart from these mode hops, the AWG laser remains in a single-mode operation regime at currents up to 200 mA and temperatures up to 60 °C.

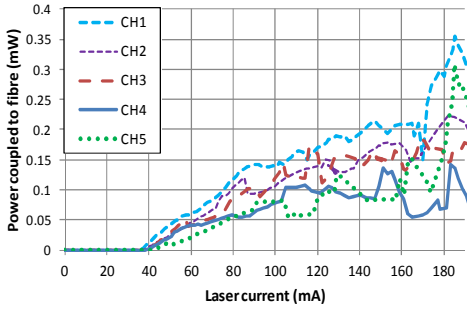

Fig 17. Power coupled to the output fibre versus injection current for each channel, at 20°C.

Figure 18 shows the temperature behaviour of the laser for channel 5 between 10 °C and 60 °C. When the temperature rises, the output power coupled to the fibre remains above 0.1 mW at a bias current of 200 mA. It is remarkable that despite the thermal insulation due to the buried oxide layer and the silica bonding layer, the laser can still operate up to 60 °C in the CW regime.

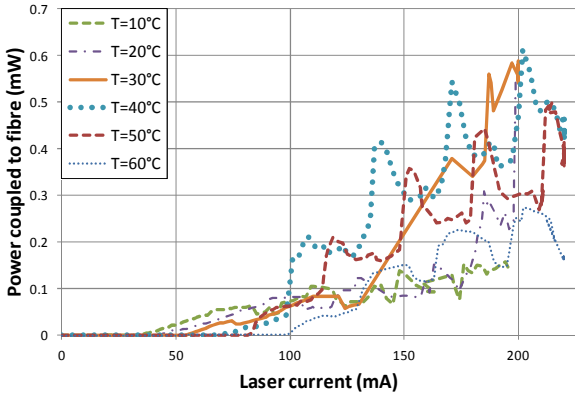

Fig 18. Power coupled to the output fibre channel 5 versus injection current, at 20 °C.

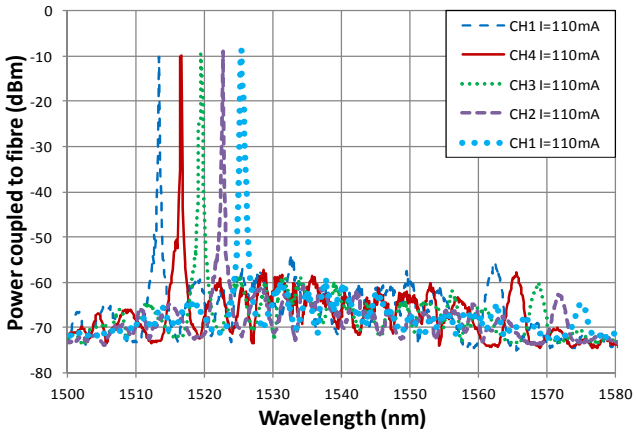

Fig 19. Superimposed laser spectra for each channel with injection current of 110mA, at 20°C.

Figure 19 shows the superimposed spectra of all 5 channels when being independently biased at 110 mA. The measurements were made using an optical spectrum analyzer. As the Fabry-Pérot modes of the AWG-laser are spaced 18 GHz apart, the spectral resolution of 0.07 nm allows to verify that each channel clearly operates in a single-mode regime with an SMSR larger than 30 dB for all channels at 110 mA. Such SMSR values are already sufficient for a number of applications, although they can still be improved in future designs by decreasing the 3 dB bandwidth of the AWG filter from the current value of 190 GHz. It is also to be noted that despite the shift between the AWG filter wavelength and the maximum of the gain curve, the SMSR limited by the AWG next order in the wavelength range 1560 nm - 1575 nm remains at least 45 dB.

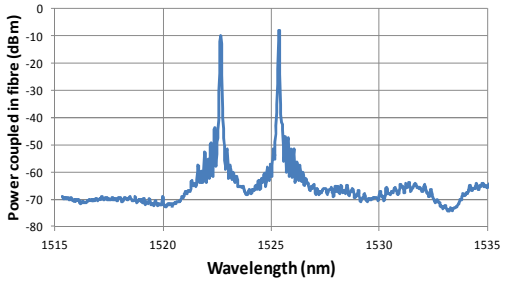

Fig 20. Spectrum of the laser with both channel 1 and 2 being switched on, with 110 mA current, at 20 °C.

Figure 20 shows the output spectrum when two channels are biased simultaneously. Both operate in a single mode regime as in the case of single channel operation. Such a behaviour shows independent operation of the two channels with negligible thermal cross-talk.

VI. Integrated Tunable Laser Mach-Zehnder Modulator

The developed ITLMZ chip consists of a single-mode hybrid III-V/silicon laser, a silicon MZM and an optical output coupler, as shown in figure 21 (top: schematic view, and bottom: a photograph). The single-mode hybrid laser includes an InP waveguide providing light amplification, and a ring resonator allowing single-mode operation. Two Bragg reflectors etched into the silicon waveguides close the laser cavity. The MZM allows modulation of the output light emitted by the hybrid laser.

In addition to the fabrication steps outlined in Sections II (hybrid III-V/Si integration) and IV (heaters), the integration of an MZM necessitates several ion implantation steps in order to realize p++, p, n and n++ dopings.

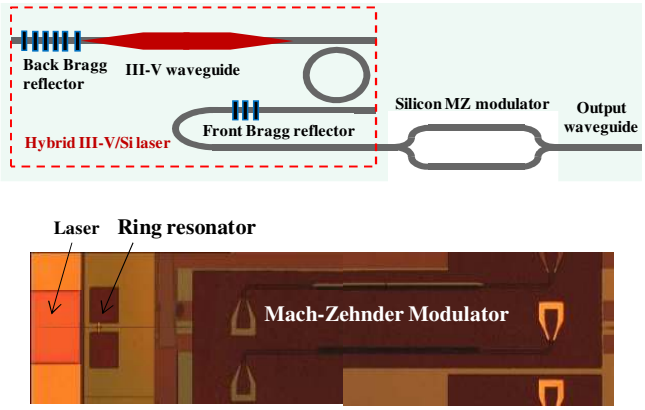

Figure 21: Schematic view (top) and picture (bottom) of the ITLMZ chip

A. *Tunable laser characteristics*

The RR-based hybrid laser exhibits a CW threshold current around 41 mA at 20°C and the output power coupled to the silicon waveguide is around 2.5 mW for an injection current of 100 mA. The maximum output power is around 6.5 mW at 20°C, and the output power is still higher than 1 mW at 60°C. Electrical current injection into the heater allows thermal tuning of the ring resonance wavelength. As a result, the selected cavity mode will jump to another one having the lowest threshold [27]. Figure 22 (top) plots the lasing wavelength as a function of the heating power. One can observe from this figure that a tuning range of 8 nm is achieved. The wavelength tuning is incremental, due to the mode jumps with the increase of heating power. This phenomenon is typical of this kind of cavity, and very similar to that observed in classical distributed feedback Bragg lasers made on InP. The heater resistance is in the range of 20-100 Ω, and the thermal tuning efficiency is in the range of 0.15–0.4 nm/mW. Figure 22 (bottom) shows an example of the superimposed optical spectra for 10 values of the heating power. Clearly, single-mode operation with SMSR larger than 40 dB is achieved.

B. *Silicon Mach-Zehnder modulator characteristics*

The silicon modulator is a depletion type lateral pn junction modulator as described in [28]. The length of the modulated phase shifters is 3 mm. The arm length difference of the MZM is 150µm, resulting in a free spectral range of around 4.5 nm. The estimated VπLπ for the modulator is around 3 V cm. The extinction ratio (ER) depends on the operation point. Its value is larger than 10 dB when the operation point is close to the minimum transmission, and 6.5 dB close to the maximum for a peak-to-peak voltage swing of 8 V. Thus the average losses are higher for the case of a larger ER. A trade-off between the losses and the ER for the modulator is made in the BER measurements. Moreover, from the power level measurement from a laser alone with the same structure and from the output of the ITLMZ chip, the intrinsic losses of the MZM are estimated to be around 13 dB at its maximum transmission point.

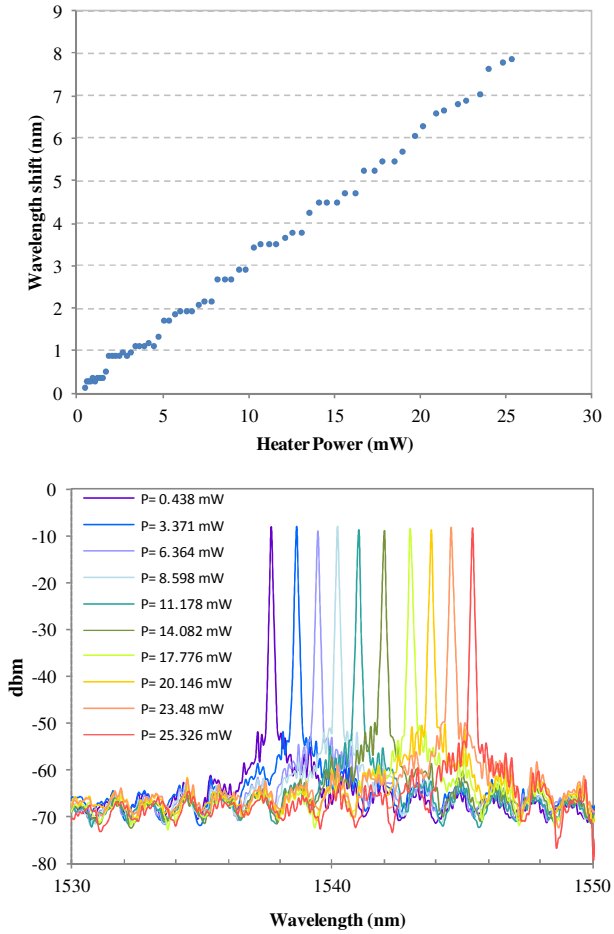

Figure 22 Lasing wavelength as a function of the heating power (top) and super-imposed optical spectra (bottom)

Figure 23 shows the small-signal modulation response of the integrated MZM for several values of the applied voltage. One can see that the modulation bandwidth increases with the rising reverse bias voltage of the pn junction due to a reduction of the capacitance with voltage. For a reverse bias larger than 2V, the 3 dB modulation bandwidth is larger than 13 GHz. The modulation response decreases very slowly with the modulation frequency. Such a modulation response guarantees operation at 10 Gb/s, and should allow modulation at bit rates up to 25 Gb/s.

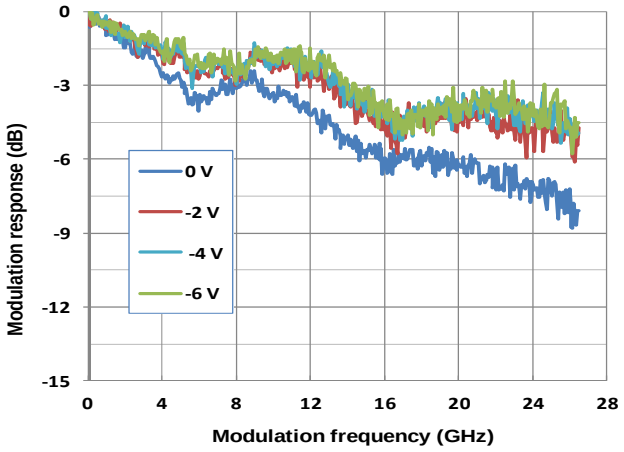

Figure 23: Small-signal modulation response of the MZ modulator for different values of the applied voltage

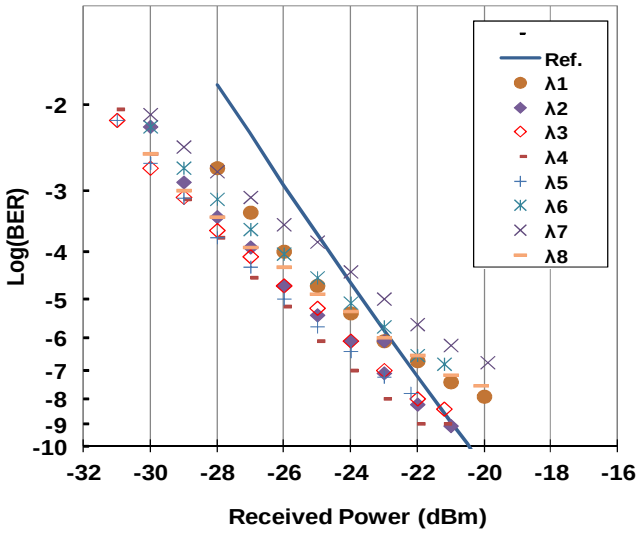

Figure 24: Bit error rate for different wavelengths

C. *BER measurement of the ITLMZ*

The output of the ITLMZ chip is coupled to a lensed fiber, amplified by an erbium doped fiber amplifier and then filtered out. One arm of the MZM is modulated with a voltage swing of around 7 V, at 10 Gb/s using a pseudo-random binary sequence (PRBS). The BER measurement is performed for 8 different wavelengths distributed inside the tuning range by changing the power dissipated in the RR heater [18]. Fig. 24 shows the BER curves for all the wavelengths and also a reference curve for a directly modulated laser, measured using a high sensitivity receiver including an avalanche photodiode. The PRBS length is 2^7-1, limited by the photo-receiver used in this experiment. Fig. 25 shows the corresponding eye diagram for all those channels, independent of the length of PRBS in the range from 2^7-1 to 2^{31}-1. The ER of the different wavelengths varies from 6 to 10 dB, while the ER for the reference is only 4 dB. One can see from Fig. 4 that all channels have better BER performance than the reference for received power levels lower than -25 dBm, due to the higher ER of the ITLMZ compared to that of the reference. For power levels higher than -25 dBm, channels λ2, λ3, λ4 and λ5 behave slightly better than the reference, achieving error-free operation with BER < 10^{-9}. Other channels have minimum BER between 10^{-7} and 10^{-8}, mainly limited by the optical signal to noise ratio (OSNR) due to the high coupling losses between the ITLMZ output waveguide and the lensed fiber used. The power level difference to achieve the same BER among all channels is around 4 dB, explained by the difference in OSNR and the achieved ER among those channels. Finally, the smaller slopes for all wavelength channels compared to that of the reference in the BER curves is attributed to their lower OSNR

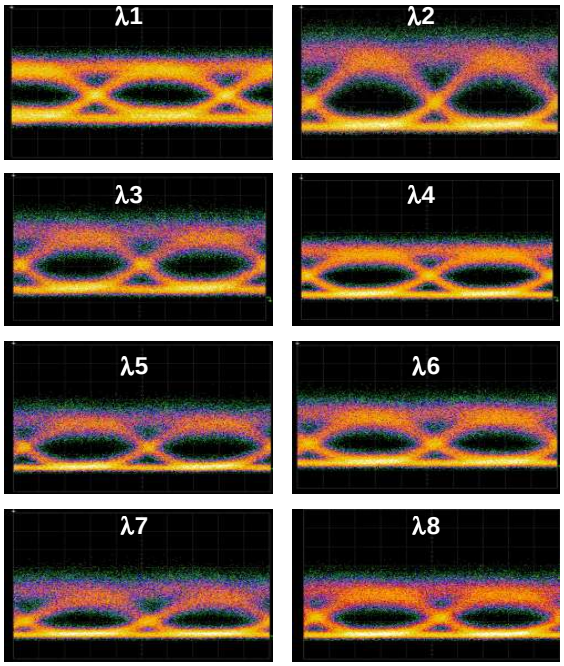

Figure 25: Eye diagrams for different wavelengths

VII. Conclusion

Heterogeneous integration of III-V on silicon seems to be a very promising way to fabricate laser sources on silicon. The performance of the fabricated III-V on silicon lasers is approaching that of a monolithically integrated InGaAsP laser on InP substrate. Moreover, the silicon waveguides allow to provide additional functionalities such as spectral filtering in a DBR laser or wavelength-tuning in lasers with integrated ring resonators. The integration of hybrid lasers on silicon further allows the fabrication of more complete photonic circuits such as transmitters and receivers. Looking into the future, we believe that the hybrid III-V on silicon lasers will find a

number of applications ranging from chip-to-chip communications to long-haul optical transmission.

REFERENCES

[1] C. Gunn, "CMOS photonics for high-speed interconnects", IEEE Proceedings of Computer Science, vol. 26, pp. 58 – 66, 2006.

[2] R. Soref, "The Past, Present, and Future of Silicon Photonics ", IEEE J. of Selected Topics on Quantum Electronics, vol. 12, No. 6 , pp. 1678 – 1687, 2006

[3] P. Dong, Y.-K. Chen, G.-H. Duan, and D. T. Neilson, "Silicon Photonic Devices and Integrated Circuits", Invited paper, to appear in J. Nanophotonics.

[4] J. F. Liu, X. Sun, R. Camacho-Aguilera, L. C. Kimerling, J. Michel, "A Ge-on-Si laser operating at room temperature", Optics Lett., vol. 35, pp. 679-681, March 2010.

[5] R. E. Camacho-Aguilera, Y. Cai, N. Patel, J. T. Bessette, M. Romagnoli, L.C. Kimerling, and J. Michel, "An electrically pumped Germanium laser", Opt. Express, vol. 20 Issue 10, pp.11316-11320, 2012

[6] A. W. Fang, H. Park, Y.-H. Kuo, R. Jones, O. Cohen, D. Liang, O. Raday, M. N. Sysak, M. J. Paniccia, J. E. Bowers, "Hybrid silicon evanescent devices", Materials Today, vol. 10, Issues 7-8, p. 28-35, 2007.

[7] G. Roelkens, J. Van Campenhout, J. Brouckaert, D. Van Thourhout, R. Baets, P. Rojo Romeo, P. Regreny, A. Kazmierczak, C. Seassal, X. Letartre, G. Hollinger, J.-M. Fedeli, L. Di Cioccio, C. Lagahe-Blanchard, "III-V/Si photonics by die-to-wafer bonding", Materials Today, vol. 10, Issues 7-8, p.36-43, 2007.

[8] H. Park, M. N. Sysak, H.-W. Chen, A. W. Fang, D. Liang, L. Liao, B. R. Koch, J. Bovington, Y. Tang, K. Wong, M. Jacob-Mitos, R. Jones, and J. E. Bowers, "Device and Integration Technology forSilicon Photonic Transm", IEEE J. of Selected Topics on Quantum Electronics,, vol. 17, No. 3, pp. 671-688, 2011.

[9] B. Ben Bakir, A. Descos, N. Olivier, D. Bordel, P. Grosse, E. Augendre, L. Fulbert, and J.-M. Fedeli, "Electrically driven hybrid Si/III-V lasers based on adiabatic mode transformers ", Optics Express, vol. 19 Issue 11, pp.10317-10325, 2011

[10] M. Lamponi, S. Keyvaninia, C. Jany, F. Poingt, F. Lelarge, G. de Valicourt, G. Roelkens, D. Van Thourhout, S. Messaoudene, J.-M. Fedeli, and G.H. Duan, "Low-threshold heterogeneously integrated InP/SOI laser with a double adiabatic taper coupler", IEEE Photonics Technology Letters, vol. 24, pp: 76 – 78, 2012.

[11] A. Le Liepvre, C. Jany, A.Accard, M. Lamponi, F. Poingt, D. Make, F. Lelarge, J.-M. Fedeli, S. Messaoudene, D. Bordel, and G.-H. Duan, "Widely Wavelength Tunable Hybrid III-V/Silicon Laser with 45 nm Tuning Range Fabricated Using a Wafer Bonding Technique", IEEE 9th International Conference on Group IV Photonics (GFP), 2012 , vol., no., pp.54-56, 29-31 Aug. 2012

[12] B. R. Koch, E. J. Norberg, B. Kim, J. Hutchinson, J.-H. Shin, G. Fish, and A. Fang, "Integrated Silicon Photonic Laser Sources for Telecom and Datacom", Proceedings of Optical Fiber Communication Conference, Post-deadline paper, Anaheim, CA, March 2013.

[13] E. Marchena, T. Creazzo, S. B. Krasulick, P. K. L. Yu, D. Van Orden, J. Y. Spann, C. C. Blivin, J. M. Dallesasse, P. Varangis, R. J. Stone, and A. Mizrahi, "Integrated Tunable CMOS Laser for Si Photonics", Proceedings of Optical Fiber Communication Conference, Post-deadline paper, Anaheim, CA, March 2013.

[14] G. Kurczveil, M. J. Heck, J. D. Peters, J. M. Garcia, D. Spencer, and J. E. Bowers, "An integrated hybrid silicon multiwavelength AWG laser," IEEE J. Sel. Topics Quantum Electron., vol. 17, no. 6, pp. 1521–1527, Nov./Dec. 2011.

[15] A. Le Liepvre, A. Accard, F. Poingt, C. Jany, M. Lamponi, D. Make, F. Lelarge, J.-M. Fedeli, S. Messaoudene, D. Bordel, and G.-H. Duan, "A wavelength selectable hybrid III-V/Si laser fabricated by wafer bonding", IEEE Photonics Technology Letters, vol. 25, No. 16, pp. 1582-1585, 2013

[16] S. Keyvaninia, S. Verstuyft, S. Pathak, F. Lelarge, G. H. Duan, D. Bordel, J. M. Fedeli, T.; De Vries, B. Smalbrugge, E.J. Geluk, J. Bolk, M. Smit, G. Roelkens, D.; Van Thourhout, "III-V-on-silicon multi-frequency lasers." Optics express, vol. 21, no. 11, pp. 13675-13683. 2013

[17] A. Alduino, et al., "Demonstration of a High Speed 4-Channel Integrated Silicon Photonics WDM Link with Hybrid Silicon Lasers", Integrated Photonics Research, Silicon and Nanophotonics (IPRSN), Monterey, CA, Postdeadline Session (IWI), 2010

[18] G-.H. Duan, C. Jany, A. Le Liepvre, J.-G. Provost, D. Make, F. Lelarge, M. Lamponi, F. Poingt, J.-M. Fedeli, S. Messaoudene, D. Bordel, S. Brision, S. Keyvaninia, G. Roelkens, D. Van Thourhout, D. J. Thomson, F. Y. Gardes and G. T. Reed, "10 Gb/s Integrated Tunable Hybrid III-V/Si Laser and Silicon Mach-Zehnder Modulator", European Conference on Optical Communication, Amsterdam, Sept. 2012.

[19] J-M. Fedeli; B. Ben Bakir; N. Olivier; Ph. Grosse; L. Grenouillet; E. Augendre; P. Phillippe; K. Gilbert; D. Bordel; and J. Harduin" InP on SOI devices for optical communication and optical network on chip", SPIE Photonic West Conference, Proceedings Vol. 7942 Optoelectronic Integrated Circuits XIII, 2011.

[20] D. Bordel, M. Argoud, E. Augendre, J. Harduin, P. Philippe, N. Olivier, S. Messaoudène, K. Gilbert, P. Grosse, B. Ben Bakir and J.-M. Fedeli., "Direct and polymer bonding of III-V to processed silicon-on-insulator for hybrid silicon evanescent lasers fabrication", ECS Transactions, 33, 403-410, 2010.

[21] A. J. Zilkie, P. Seddighian, B. J. Bijlani, W. Qian, D. C. Lee, S. Fathololoumi, J. Fong, R. Shafiiha, D. Feng, B. J. Luff, X. Zheng, J. E. Cunningham, A. V. Krishnamoorthy, and M. Asghari, "Power-efficient III-V/Silicon external cavity DBR lasers," Opt. Express vol. 20, pp. 23456-23462, 2012.

[22] G. de Valicourt, A. Leliepre, F. Vacondio, C. Simonneau C. Jany, A. Accard, F. Lelarge, M. Lamponi, D. Make, F. Poingt, G. H. Duan, J.-M. Fedeli, S. Messaoudene, D. Bordel, L. Lorcy, J.-C. Antona and S. Bigo, "Directly modulated and fully tunable hybrid silicon lasers for future generation of coherent colorless ONU", Opt. Express, vol. 20, B552-B557, 2012.

[23] M. Zirngibl, C. H. Joyner, C. R. Doerr, L. W. Stultz, and H. M. Presby, "An 18-channel multifrequency laser", IEEE Photon. Technol. Lett., vol. 8, pp.870 -872 1996

[24] A. Staring, L. Spiekman, J. J M. Binsma, E. J. Jansen, T. Van Dongen, P. J. A. Thijs, M. K. Smit, and B. H. Verbeek,"A compact nine-channel multiwavelength laser," Photonics Technology Letters, IEEE , vol.8, no.9, pp.1139,1141, Sept. 1996

[25] W. Bogaerts, P. Dumon , D. V. Thourhout, D. Taillaert, P. Jaenen, J. Wouters, S. Beckx, V. Wiaux, R. G. Baets, "Compact Wavelength-Selective Functions in Silicon-on-Insulator Photonic Wires," IEEE Journal of Selected Topics in Quantum Electronics, , vol.12, no.6, pp.1394-1401, Nov.-dec. 2006

[26] M. J. R. Heck, A. La Porta, X. J. M. Leijtens, L. M. Augustin, T. De Vries, B. Smalbrugge, O. Yok-Siang, R. Notzel, R. Gaudino, D. J. Robbins, M. K. Smit, "Monolithic AWG-based Discretely Tunable Laser Diode With Nanosecond Switching Speed," IEEE Photonics Technology Letters, vol.21, no.13, pp.905,907, July1, 2009

[27] S. Keyvaninia, G. Roelkens, D. Van Thourhout, C. Jany, M. Lamponi, A. Le Liepvre, F. Lelarge, D. Make, G. Duan, D. Bordel, and J. Fedeli, "Demonstration of a heterogeneously integrated III-V/SOI single wavelength tunable laser," Opt. Express 21, 3784-3792, 2013.

[28] D. J. Thomson, F. Y. Gardes, Y. Hu, G. Mashanovich, M. Fournier, P. Grosse, J.-M. Fedeli, G. T. Reed, "High contrast 40Gbit/s optical modulation in silicon," Opt. Express, vol. 19, pp. 11507-11516, 2011.

Guang-Hua Duan (S'88–M'90–SM'01) received the B. E. degree in 1983 from Xidian University, Xi'an, China, the M. E. and Doctorate degrees in 1987 and 1991 respectively, both from the Ecole Nationale Supérieure des Télécommunications (Telecom-ParisTech), France, all in applied physics. He was habilitated to direct researches by Université de Paris-Sud in 1995. He is now the leader of the research team "Silicon Photonics" within III-V Lab, which is a joint Joint laboratory of "Alcatel-Lucent Bell Labs France", "Thales Research and Technology" and "CEA Leti". He is

author or co-author of more than 100 journal papers, 200 conference papers, 25 patents and a contributor to 3 book chapters. He is also a Guest Professor in Ecole Supérieure d'Elecricité, and Ecole Supérieure d'Optique, giving lectures in the fields of electromagnetism, optoelectronics and laser physics.

Christophe JANY received the Ph.D. degree in materials science from the University of Paris XII, France, in 1998. He studied thin film technology of CVD Diamond on Silicon. He joined Alcatel Research & Innovation Center in Marcoussis in 1999. He has been engaged in the development of optical integration technology of III-V semiconductors components, including high speed (> 40 Gb/s) integrated lasers and electro-absorption modulators. Within Bell Labs France, he contributed to the development of new InP-based platforms integration using SAG and SIBH Technologies. So, he is now with III-V Lab, leading expert in the field of photonic integration with over 13 years of experience in the field of InP-based Photonic Integrated Circuits (PICs). For 3 years, he develops the hybrid technology III-V on SOI, leading to the Silicon Photonics chips (Laser source). He main focuses to make compatible manufacturing III-V materials on 'CMOS' material.

Marco Lamponi was born in Terni, Italy, in 1984. He received the M.Sc. degree in physical engineering from the Politecnico di Milano, Milan, Italy, and the French diploma of electrical engineering from the Ecole Superieure d'Electricite of Paris, France, in 2008. He received the M.Sc. degree in nano-science and micro-systems and the Ph.D. degree from Paris-sud University, Orsay, France, in 2012. His doctoral work focused on the design and fabrication of hybrid III-V on silicon lasers. He got a permanent position in January 2012 at III-V Lab, Palaiseau, France, to work on III-V photonic integrated circuits and high power lasers.

Peter Kaspar received the M.Sc. and Ph.D degree in physics from ETH Zurich, Switzerland, in 2005 and 2012, respectively. In 2005, he was with the Ultrafast Laser Physics Laboratory, ETH Zurich, where he worked on high harmonic generation in noble gases using ultrashort laser pulses. From 2006 to 2012 he was with the Communication Photonics Group, Electronics Laboratory, ETH Zurich, where he studied nanostructured photonic elements and developed III–V semiconductor technology for active photonic crystal devices. He joined III-V Lab, Palaiseau, France, in 2013 to work on hybrid lasers and SOAs (III-V on silicon) for photonic integrated circuits on silicon.

Guillaume Levaufre received a Master's degree of Engineering in opto-electronics from INSA Rennes, France, in 2012. The same year, he made an internship at the III-V Lab, working on inductively coupled plasma etching of InP. Since October 2012, he has joined Alcatel-Lucent Bell Labs as a PhD student at III-V Lab. His research work is focused on hybrid III-V/Silicon photonic integrated circuits for high-speed telecommunications.

Nils Girard received a Master's degree of Engineering (option: Photonics) from SUPELEC and a Master of Science (Physics, Plasma, Photonics) from the University of Metz-Nancy in 2012. Later this year, he worked with Thales Research and Technology on the generation of RF signal with dual-frequency VECSEL. He started a Ph.D with the III-V Lab, Palaiseau, France in November 2012 to work on Low Noise Hybrid III-V/Silicon lasers for radar and ultra stable clocks applications.

François Lelarge received the Diploma in material science in 1993 and the Ph. D degree in 1996, both from the University of Pierre et Marie Curie, Paris, France. From 1993 to 1996, he was with the Laboratory of Microstructures and Microelectronic, CNRS Bagneux, France. His thesis work was devoted to the fabrication and the optical characterization of GaAs/AlAs lateral supperlattice grown on vicinal surfaces by MBE. From 1997 to 2000, he was a post-doctoral Researcher at the Institute of Micro and Optoelectronics, Lausanne, Switzerland. He worked on InGaAs/GaAs quantum wires fabrication by MOCVD regrowth on patterned substrates. Presently, he is in charge of the Epitaxy and New Material Technology team within III-V Lab and coordinator of a project on QD-based directly modulated lasers (ANR-DIQDOT).

Guilhem de Valicourt received the BSc degree in applied physics from the National Institute of applied Sciences (INSA), Toulouse, France, in 2008. From 2007 to 2008, he followed and passed the Master of Science in Photonics Devices at Essex University, U.K. In 2008, he joined III-V lab where he was working on design, fabrication, and characterization of Reflective SOA and directly modulated DFB lasers for microwave photonic systems and next generation of optical access networks toward the Ph.D. In 2011 he joined Alcatel-Lucent Bell Labs in France as a research engineer. His main research interests are focused on the study of advanced integrated photonics devices (in InP, silicon and hybrid III-V on silicon platform) for optical packet transport and switching for metropolitan and wireless backhaul networks as well as for datacenters and access networks. He has authored or co-authored more than 50 scientific papers in journals and international conferences, 2 book chapters and holds 15 patents. I received the 2011 "Best project" award from Alcatel-Lucent Bootcamp, the Marconi Young Scholar 2012 award and was finalist for the ParisTech PhD prize 2012.

G. Roelkens graduated in 2002 as an electronics engineer (option: micro-electronics and opto-electronics) from Ghent University (with highest honour). Since 2002, he has been working in the Photonics Research Group at Ghent University,

where he received the doctoral degree in April 2007, for his work in the field of heterogeneous III-V/Silicon photonics. In this work, the technology for integrating III-V material on top of silicon-on-insulator waveguide circuits was developed and the integration of thin film III-V laser diodes and photodetectors on top of and coupled to the SOI waveguide circuit was demonstrated. Now he is working as tenure track professor in the same group. His research interests include heterogeneous III-V/silicon integration, efficient fiber-chip coupling, all-optical signal processing and mid-infrared photonic integrated circuits.

David J. Thomson is a senior research fellow in the Optoelectronics Research Centre (ORC) at the University of Southampton. His research interests are optical modulation, optical switching, integration and packaging in silicon. He started his silicon photonics research in 2004 as a PhD student at the University of Surrey under the guidance of Prof. Graham Reed. His PhD project involved investigating silicon based total internal reflection optical switches and more specifically methods of restricting free carrier diffusion within such devices. In 2008 he took up a role as a research fellow in the same research group leading the work package on silicon optical modulators within the largest European silicon photonics project named HELIOS. Within this project David designed the first silicon optical modulator operating at 50Gbit/s. In 2011 David presented invited talks at SPIE Photonics West and IEEE Group IV Photonics conferences and in 2012 was selected to present his work at the SET for Britain event in the Houses of Parliament.

Frederic Y. Gardes is an Academic Fellow appointed as a lecturer at the University of Southampton in the Electronics and computer science department (ECS); he is conducting his research as part of the Optoelectronics Research Centre (ORC). Gardes previous research covers silicon photonics and particularly high speed active optical devices in silicon and germanium. In 2005 Gardes initiated work on silicon optical depletion modulators and was the first to predict operation above 40GHz. In 2011 Gardes and his collaborators demonstrated optical modulation of up 50 Gb/s and a 40Gb/s modulator with a quadrature Extinction Ratio (ER) of 10dB setting a new state of the art performance in both speed of modulation in silicon devices and extinction ratio. Gardes is currently working with several national and international collaborators in two large research programs where he leads the research effort in optical modulators and detector integration. These programmes are the £5M UK Silicon Photonics project funded by EPSRC, and the £8M EU FP7 HELIOS. Gardes is also involved in photonic crystal slow light, ultra-low power nano-cavity modulators, Silicon/Germanium QCSE devices, Germanium and defect induced detectors in silicon and active device integration in group IV materials. Gardes has authored more than 80 publications and 5 book chapters in the field of Silicon Photonics. He has also been involved in the FP6 ePIXnet program and is a regular invited and contributing author to the major Silicon Photonics conferences around the world. Gardes is also a member of the programme committee of the IEEE Group IV Photonics conference.

Graham Reed is Professor of Silicon Photonics and Group Leader. He has recently joined Southampton from the University of Surrey, where he was Professor of Optoelectronics, and was Head of the Department of Electronic Engineering from 2006 to 2012. Reed is a pioneer in the field of Silicon Photonics, and acknowledged as the individual who initiated the research field in the UK. He established the Silicon Photonics Research Group at Surrey in 1989. The first Silicon Photonics company in the world, Bookham Technology Inc., was founded by Reed's PhD student, Dr Andrew Rickman, and adopted the research developed in the Group. The Silicon Photonics Group have provided a series of world leading results since it's inception, and are particularly well known for their work on silicon optical modulators. For example, the Group produced the first published design of an optical modulator with a bandwidth exceeding 1 GHz, and were the first to publish the design of a depletion mode optical modulator, which is now a technology standard device. More recently the team were responsible for the first all-silicon optical modulator operating at 40Gb/s with a high extinction ratio (10dB), as well as a second modulator design (also operating at 40Gb/s) that operates close to polarization independence. They have now reported the first device operating at 50 Gb/s. Reed is a regular invited and contributing author to the major Silicon Photonics conferences around the world. He has served on numerous international conference committees, and has also chaired many others. To name but two, he has been co-chair, of the Silicon Photonics symposium at Photonics West since it was first established in 2006, and in 2011 he was co-chair of the prestigious Silicon Photonics conference, IEEE Group IV Photonics, held at the Royal Society in London. He is currently a member of 5 international conference committees, and has published over 250 papers in the field of Silicon Photonics. He will co-chair 4 international symposia/conferences in 2012.